

23. K. Uosaki, T. Kondo, H. Noguchi, K. Murakoshi, and Y. Y. Kim, *J. Phys. Chem.*, **100**, 4564 (1996).
24. E. S. Kooij, A. R. Rama, and J. J. Kelly, *Surf. Sci.*, **370**, 125 (1997).
25. L. M. Peter, D. J. Blackwood, and S. Pons, *Phys. Rev. Lett.*, **62**, 308 (1989).
26. J.-N. Chazalviel and F. Ozanam, *J. Appl. Phys.*, **81**, 7684 (1997).
27. L. M. Peter, Private communication.
28. R. Memming, *J. Electrochem. Soc.*, **116**, 785 (1969).
29. H. J. H. Fenton, *J. Chem. Soc.*, **65**, 899 (1894).
30. F. Haber and J. J. Weiss, *Proc. Roy. Soc. London, Ser. A*, **147**, 332 (1934).
31. M. J. Madou, B. H. Loo, K. W. Frese, and S. R. Morrison, *Surf. Sci.*, **108**, 135 (1981).
32. A. J. Bard, R. Parsons, and J. Jordan, *Standard Potentials in Aqueous Solutions*, Marcel Dekker, New York (1985).
33. O. M. R. Chyan, J.-J. Chen, L. Chen, and F. Xu, *J. Electrochem. Soc.*, **144**, L17 (1997).
34. B. Gelloz, A. Bsiesy, F. Gaspard, R. Herino, M. Ligeon, F. Muller, R. Romestain, and J. C. Vial, in *Pits and Pores: Formation, Properties, and Significance for Advanced Luminescent Materials*, P. Schmuki, D. J. Lockwood, H. Isaacs, A. Bsiesy, Editors, p 422, PV 97-7, The Electrochemical Society Proceedings Series, Pennington, NJ (1997).
35. A. Bsiesy, J. C. Vial, F. Gaspard, R. Herino, M. Ligeon, I. Mihalcescu, F. Muller, and R. Romestain, *J. Electrochem. Soc.*, **141**, 3071 (1994).
36. E. A. Meulenkaamp, L. M. Peter, D. J. Riley, and R. I. Wielgosz, *J. Electroanal. Chem.*, **392**, 97 (1995).

# LiMn<sub>2-x</sub>Cu<sub>x</sub>O<sub>4</sub> Spinel (0.1 ≤ x ≤ 0.5): A new Class of 5 V Cathode Materials for Li Batteries

## I. Electrochemical, Structural, and Spectroscopic Studies

Yair Ein- Eli,\* W. F. Howard, Jr.,\* and Sharon H. Lu

Covalent Associates, Incorporated, Woburn, Massachusetts 01801, USA

Sanjeer Mukerjee\* and James McBreen\*

Brookhaven National Laboratory, Upton, New York 11973-5000, USA

John T. Vaughan and Michael M. Thackeray\*

Argonne National Laboratory, Argonne, Illinois 60439, USA

### ABSTRACT

A series of electroactive spinel compounds, LiMn<sub>2-x</sub>Cu<sub>x</sub>O<sub>4</sub> (0.1 ≤ x ≤ 0.5), has been studied by crystallographic, spectroscopic, and electrochemical methods and by electron microscopy. These LiMn<sub>2-x</sub>Cu<sub>x</sub>O<sub>4</sub> spinels are nearly identical in structure to cubic LiMn<sub>2</sub>O<sub>4</sub> and successfully undergo reversible Li intercalation. The electrochemical data show a remarkable reversible electrochemical process at 4.9 V which is attributed to the oxidation of Cu<sup>2+</sup> to Cu<sup>3+</sup>. The inclusion of Cu in the spinel structure enhances the electrochemical stability of these materials upon cycling. The initial capacity of LiMn<sub>2-x</sub>Cu<sub>x</sub>O<sub>4</sub> spinels decreases with increasing x from 130 mAh/g in LiMn<sub>2</sub>O<sub>4</sub> (x = 0) to 70 mAh/g in "LiMn<sub>1.5</sub>Cu<sub>0.5</sub>O<sub>4</sub>" (x = 0.5). The data also show slight shifts to higher voltage for the delithiation reaction that normally occurs at 4.1 V in standard Li<sub>1-x</sub>Mn<sub>2</sub>O<sub>4</sub> electrodes (1 ≥ x ≥ 0) corresponding to the oxidation of Mn<sup>3+</sup> to Mn<sup>4+</sup>. Although the powder X-ray diffraction pattern of "LiMn<sub>1.5</sub>Cu<sub>0.5</sub>O<sub>4</sub>" shows a single-phase spinel product, neutron diffraction data show a small but significant quantity of an impurity phase, the composition and structure of which could not be identified. X-ray absorption spectroscopy was used to gather information about the oxidation states of the manganese and copper ions. The composition of the spinel component in the LiMn<sub>1.5</sub>Cu<sub>0.5</sub>O<sub>4</sub> was determined from X-ray diffraction and X-ray absorption near-edge spectroscopy to be Li<sub>1.01</sub>Mn<sub>1.67</sub>Cu<sub>0.32</sub>O<sub>4</sub>, suggesting to a best approximation that the impurity in the sample was a lithium-copper-oxide phase. The substitution of manganese by copper enhances the reactivity of the spinel structure toward hydrogen: the compounds are more easily reduced at moderate temperature (~200°C) than LiMn<sub>2</sub>O<sub>4</sub>.

### Introduction

Materials that reversibly intercalate lithium form the cornerstones of the emerging lithium-ion battery industry. Lithiated graphite and pyrolyzed carbons<sup>1,2</sup> and more recently, glassy tin oxides,<sup>3</sup> are the anodes of greatest interest as they offer a low potential vs. lithium, typically below 1 V. Layered rock-salt compounds such as LiCoO<sub>2</sub> and LiNiO<sub>2</sub><sup>4,5</sup> are proven 4 V cathode materials.<sup>6-8</sup> Currently, LiCoO<sub>2</sub> is the preferred electrode material for commercial lithium-ion batteries<sup>9</sup> which are now being manufactured at a rate of 250 million units/year.<sup>10</sup> Nonetheless, Co and Ni compounds have economic and environmental problems that leave the door open to exploit alternative materials.

The spinel LiMn<sub>2</sub>O<sub>4</sub> is an inexpensive, environmentally benign intercalation cathode that is the subject of intense development,<sup>11</sup> although it is not without faults. The achiev-

able electrode capacity (120 mAh/g) is 15-30% lower than that which can be obtained from Li(Co,Ni)O<sub>2</sub> cathodes. Moreover, an unmodified LiMn<sub>2</sub>O<sub>4</sub> electrode exhibits an unacceptably high capacity fade. Several researchers have stabilized the LiMn<sub>2</sub>O<sub>4</sub> electrode structure to lithium insertion/extraction reactions at ~4 V by substituting a small fraction (~2.5%) of the manganese ions with other metal cations.<sup>12-14</sup> Although these substitution techniques can successfully combat the capacity decline at 4 V, the initial reversible capacity is no better than 115 mAh/g.<sup>14</sup>

Extending the concept of Mn replacement in the spinel, Davidson et al.<sup>15</sup> and Amine et al.<sup>16</sup> have used Cr and Ni, respectively, to produce LiMn<sub>2-x</sub>M<sub>x</sub>O<sub>4</sub> electrodes (x ≈ 0.5) that provide improved stability to electrochemical cycling at 3 V. Guyomard and co-workers<sup>17</sup> showed that lithium extraction from the Cr-substituted spinel occurs at 4 and 4.9 V; these reactions were attributed to the oxidation of manganese and chromium, respectively. Gao et al.<sup>18</sup> dis-

\* Electrochemical Society Active Member.

covered that lithium extraction from  $\text{LiMn}_{1.5}\text{Ni}_{0.5}\text{O}_4$  occurs at 4.7 V, attributing this reaction to the oxidation of  $\text{Ni}^{2+}$  to  $\text{Ni}^{4+}$ .

Recently, we reported a preliminary account of the preparation and electrochemical behavior of a copper-substituted spinel,  $\text{LiMn}_{1.5}\text{Cu}_{0.5}\text{O}_4$ .<sup>19</sup> In this paper, we present electrochemical, structural, and spectroscopic data obtained from an examination of various compounds in the  $\text{LiMn}_{2-x}\text{Cu}_x\text{O}_4$  system ( $0 \leq x \leq 0.5$ ) which provide a much greater understanding of the behavior of these materials than initially reported.<sup>19</sup> Structural properties and variations in the cation charge distribution are used to explain the electrochemical behavior of  $\text{LiMn}_{2-x}\text{Cu}_x\text{O}_4$  electrodes. X-ray absorption studies were used to determine the oxidation states of the manganese and copper ions. The sample, which was two-phase, consisted of a predominant spinel phase and a lithium-copper-oxide phase. The structure of the spinel component, as determined by a Rietveld refinement of the powder X-ray diffraction pattern, is presented. The influence of copper on the reactivity of the spinel structure toward hydrogen has been studied by thermogravimetric analysis.

### Experimental

$\text{LiMn}_{2-x}\text{Cu}_x\text{O}_4$  ( $0 \leq x \leq 0.5$ ) cathode materials were prepared by conventional solid-state and sol-gel methods. In the solid-state syntheses,  $\text{LiOH} \cdot \text{H}_2\text{O}$  was mixed intimately with the required amounts of  $\text{CuO}$  and  $\text{MnO}_2$  for a given stoichiometry and then heated for 18 h in air at 750°C. The product was free-flowing and did not require milling.

Nearly phase-pure  $\text{LiMn}_{1.5}\text{Cu}_{0.5}\text{O}_4$  was prepared by a sol-gel process by dissolving stoichiometric amounts of  $\text{CH}_3\text{COOLi}$  (Acros),  $\text{Cu}(\text{OOCCH}_3)_2 \cdot \text{H}_2\text{O}$  (Avocado), and  $\text{Mn}(\text{OOCCH}_3)_2$  (Aldrich) in deionized water and adding a 4-times molar amount of  $\text{NH}_4\text{OH}$ . The mixture was stirred with gentle heating for 2 h and then concentrated to dryness on a rotary evaporator. The powdered precursor was divided into four samples which were treated at different temperatures as outlined in the Discussion section. Elemental analyses, undertaken by Laboratory Testing (Dublin, PA) confirmed the composition of the final materials.

Cyclic voltammograms were obtained with an EG&G Princeton Applied Research potentiostat model 263A; they were recorded at a slow sweep rate of 15  $\mu\text{V}/\text{s}$ . Cycling data were collected on either a Maccor series 4000 or Starbuck multichannel cyclers. Cathode materials were studied with a lithium foil anode (10 mil, Cyprus Foote Mineral) separated with Whatman BS-65 glass microfibers in a 1  $\text{cm}^2$  parallel-plate configuration. Cathode films were prepared from a slurry of  $\text{LiCu}_x\text{Mn}_{2-x}\text{O}_4$  with 10% PVDF (polyvinylidene fluoride, Atochem, North America) and 10% acetylene black (w/w) dissolved in *N*-methyl-2-pyrrolidinone (NMP, Aldrich). The mixture was doctor-bladed onto aluminum foil, dried at 140°C under vacuum for several hours, then roll-compressed at 100 atm. Cathode disks (1  $\text{cm}^2$ ) were then punched from the sheet, with an average weight of 6 mg of active material. Cell assembly was carried out under an Ar atmosphere. The electrolyte composition was 1.2 M  $\text{LiPF}_6$  (Hashimoto Chemical) in a mixture of ethylene carbonate (EC) and dimethyl carbonate (DMC) (EM Industries and Mitsubishi Chemical) in a volume ratio of 2EC:3DMC. This electrolyte was selected because of its reported stability to oxidation up to 5 V.<sup>19</sup> Cells were charged and discharged galvanostatically at a current density of 0.25  $\text{mA}/\text{cm}^2$  between 3.3 and 5.1 V.

Samples were prepared for X-ray absorption spectroscopy by mixing  $\text{LiCu}_{0.5}\text{Mn}_{1.5}\text{O}_4$  with BN and pressing it into a thin wafer. X-ray absorption data were collected with the storage ring operating 2.584 GeV and an electron current between 110 and 350 mA. The monochromator was operated in the two-crystal mode with  $\text{Si}(111)$  crystals. The monochromator was detuned by 50% at the Mn edge and by 15% at the Cu edge to reject higher harmonics. The experiments were carried out in the transmission mode with three detectors. The third detector was used in conjunction with a reference sample, which was either a Cu

foil or a polymer bonded Mn powder sample. In this way, the edge positions of the spectra could be calibrated. Other details of the measurements have been published.<sup>20</sup> Because our primary interest was the determination of the oxidation state of the Mn and Cu ions, only the X-ray absorption near-edge fine structure (XANES) was analyzed in detail. The methods used in analyzing the XANES data are described in detail elsewhere.<sup>21</sup> Data were also obtained on several compounds of copper and manganese with known oxidation states.

A Philips 1840 diffractometer with  $\text{Fe K}\alpha$  radiation was used to obtain powder X-ray diffraction patterns to characterize the samples. For the detailed structure analyses, X-ray diffraction data of two independent powder samples of  $\text{LiCu}_{0.5}\text{Mn}_{1.5}\text{O}_4$  were collected on an automated Siemens D5000 diffractometer with  $\text{Cu K}\alpha$  radiation between 15 and 120° 2 $\theta$ . The X-ray patterns of these samples showed a single-phase spinel product. By contrast, neutron diffraction data of these two samples collected by the intense pulsed neutron source (IPNS) at Argonne National Laboratory and by the high-resolution powder diffractometer (HRPD) at the Rutherford Laboratory (U.K.) showed evidence of a small but significant impurity phase that could not be identified. Because of problems encountered with a two-phase refinement of the neutron data, a best approximation of the structure of the spinel component was determined from the X-ray data by the Rietveld profile refinement technique with the software package GSAS.<sup>22</sup>

Thermogravimetric analyses were performed by Springborn Testing & Research (Enfield, CT) with a DuPont 9000 thermal analyzer equipped with a DuPont 951 thermogravimetric analyzer. The samples were analyzed from 30 to 900°C at 5°C/min under hydrogen with a flow rate of 40  $\text{mL}/\text{min}$ .

### Results and Discussion

**Sample preparation.**—Attempts to prepare  $\text{LiMn}_{2-x}\text{Cu}_x\text{O}_4$  cathode materials via conventional solid-state reaction techniques resulted in persistent  $\text{Mn}_2\text{O}_3/\text{Li}_2\text{MnO}_3$  impurities in the products, whereas sol-gel methods produced purer materials. The X-ray diffraction patterns of typical products (obtained with  $\text{Fe K}\alpha$  radiation) made by the two routes are shown in Fig. 1. Three subsequent firings of the products made by the solid-state reaction route reduced the  $\text{Mn}_2\text{O}_3/\text{Li}_2\text{MnO}_3$  impurity levels only marginally. For the sol-gel route, the powdered precursor described in the Experimental section was divided into four lots heated for 18 h in air at 350, 500, 650, and 750°C, respectively. Figure 2 shows the X-ray diffraction patterns of  $\text{LiMn}_{1.5}\text{Cu}_{0.5}\text{O}_4$  samples after the first firing step at various temperatures. Even at a preparation temperature of 350°C, there is evidence of spinel formation, although  $\text{Mn}_2\text{O}_3$  is still prevalent as an impurity phase at this temperature. At higher temperatures, the impurity levels of  $\text{Mn}_2\text{O}_3$  decrease and the spinel peaks sharpen and increase in intensity, indicative of

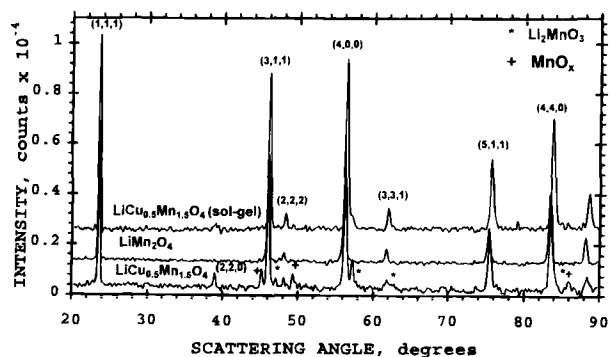


Fig. 1. XRD patterns obtained from  $\text{LiCu}_{0.5}\text{Mn}_{1.5}\text{O}_4$  spinel prepared by solid-state and sol-gel preparation methods. The XRD pattern of unmodified  $\text{LiMn}_2\text{O}_4$  spinel is shown for comparison.

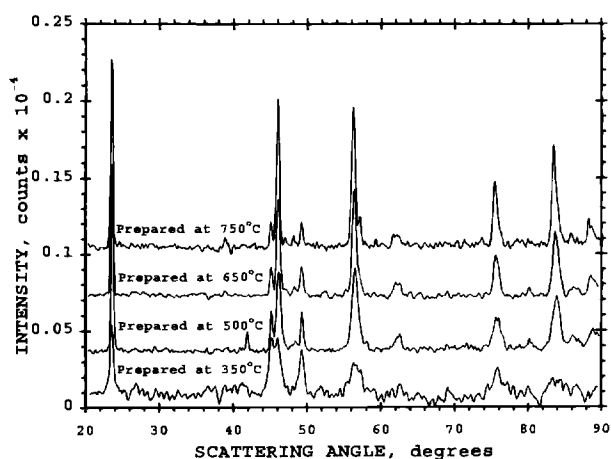


Fig. 2. XRD patterns obtained from  $\text{LiCu}_{0.5}\text{Mn}_{1.5}\text{O}_4$  prepared via the sol-gel method at one calcining temperature.

an increase in crystallinity. Note that  $\text{Li}_2\text{MnO}_3$  appears only in the 750°C sample in very minor concentration.

The  $\text{LiMn}_{1.5}\text{Cu}_{0.5}\text{O}_4$  samples prepared at 350 and 500°C were each subsequently refired at 650 and 750°C. The X-ray diffraction patterns of these materials are shown in Fig. 3 and 4, respectively. Refiring at 650°C resulted in the incorporation of most of the unreacted manganese oxides into the spinel structure; a final 750°C soak was necessary to complete the reaction. This firing sequence produced what appeared to be essentially phase-pure materials (Fig. 1 and 4); the X-ray data show a small but significant

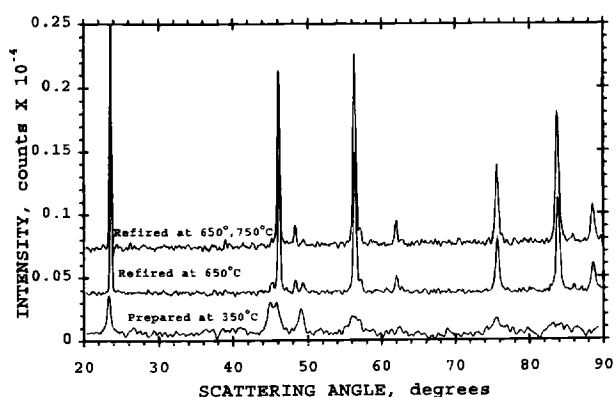


Fig. 3. XRD patterns of  $\text{LiCu}_{0.5}\text{Mn}_{1.5}\text{O}_4$  prepared via the sol-gel method with calcining temperature of 350°C which was subsequently refired at 650 and 750°C.

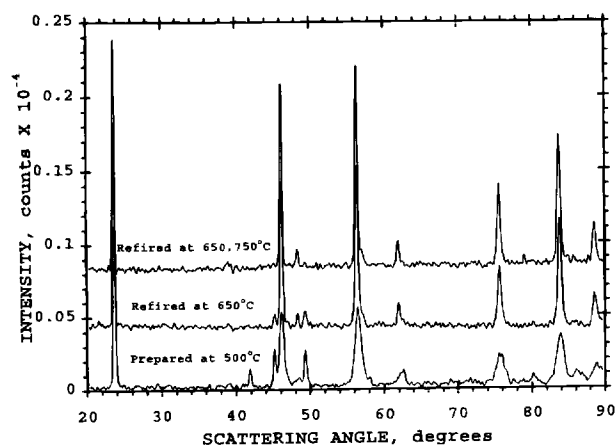


Fig. 4. The same as Fig. 3, calcining temperature 500°C.

[220] peak at 39° 2θ. The intensity of this peak indicates that a small amount of copper resides on the 8a tetrahedral sites of the spinel structure.

The neutron diffraction pattern of a  $\text{LiMn}_{1.5}\text{Cu}_{0.5}\text{O}_4$  sample is shown in Fig. 5. The data show clear evidence for the presence of a spinel phase (solid line) and an impurity phase (dotted line). The peaks of the impurity phase are also highlighted by an expanded region of the data (inset in Fig. 5) and the difference profile, shown below the neutron diffraction pattern, which was obtained by subtracting the spinel peaks from the pattern. The composition of the spinel component in the sample as determined by X-ray diffraction analysis (described in a following section) indicated that the impurity phase was a lithium-copper-oxide compound. The appearance of the impurity only in the neutron diffraction pattern was attributed to the fact that copper is a very strong scatterer of neutrons ( $b = 0.78 \times 10^{12} \text{ \AA}$ ). The observation of the impurity phase only in the neutron diffraction pattern highlights the possible dangers of misinterpreting X-ray diffraction patterns.

**Electrochemical studies.**—The potential limits that were used for the electrochemical cycling of  $\text{Li}/\text{LiMn}_{2-x}\text{Cu}_x\text{O}_4$  cells were 3.3–5.1 V. In general, the charge capacity of the spinel electrode exceeded the discharge capacity by 5–10% during the first 10 cycles; this coulombic inefficiency was attributed to slight electrolyte oxidation at the higher potentials. Figure 6 shows the voltage profiles obtained for the various  $\text{Li}/\text{LiMn}_{2-x}\text{Cu}_x\text{O}_4$  cells ( $0 \leq x \leq 0.5$ ) during the

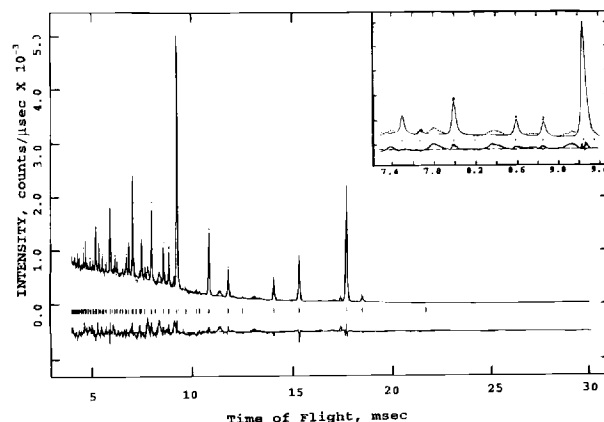


Fig. 5. Refined neutron diffraction pattern for  $\text{Li}_{1.01}[\text{Mn}_{1.67}\text{Cu}_{0.32}]\text{O}_4$ . The data are shown as small dots, the calculated pattern (based on the reported model) is shown as a solid line, and the difference between the calculated and observed data is shown below the diffraction pattern. The inset in the upper right corner shows in more detail the region from 7.3 ms, and the impurity phase in the material can be clearly seen in the difference profile. The tick marks in the spectra identify the peaks from the spinel phase.

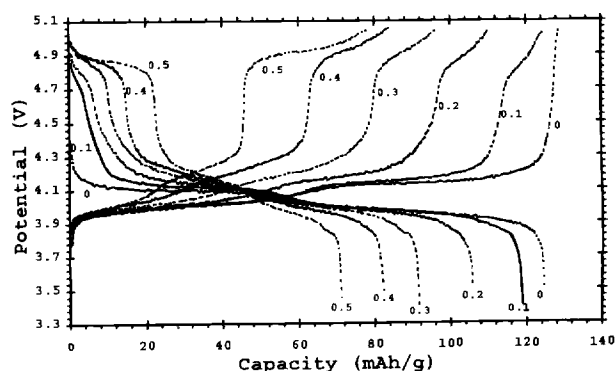


Fig. 6. The potential (V)-capacity (mAh/g) curves obtained from the third cycle for  $\text{LiCu}_x\text{Mn}_{2-x}\text{O}_4$  ( $0 \leq x \leq 0.5$ ) in steps of  $x = 0.1$ . Li metal served as counter electrode in EC(2):DMC(3)/1.2 M  $\text{LiPF}_6$ .

**Table I. Relative capacities of empirical "LiCu<sub>x</sub>Mn<sub>2-x</sub>O<sub>4</sub>" electrodes.**

$x$ in LiCu <sub>x</sub> Mn <sub>2-x</sub> O <sub>4</sub>	Capacity, mAh/g at 5.1–4.5 V	Capacity, mAh/g at 4.5–3.3 V	Cu:Mn capacity ratio
0.1	7	112	1:16
0.2	10	96	1:10
0.3	13	79	1:6
0.4	19	63	1:3
0.5	23	48	1:2

third cycle. The total capacity of LiMn<sub>2-x</sub>Cu<sub>x</sub>O<sub>4</sub> electrodes drops with increasing copper content from 119 mAh/g at  $x = 0.1$  to 71 mAh/g at  $x = 0.5$ .

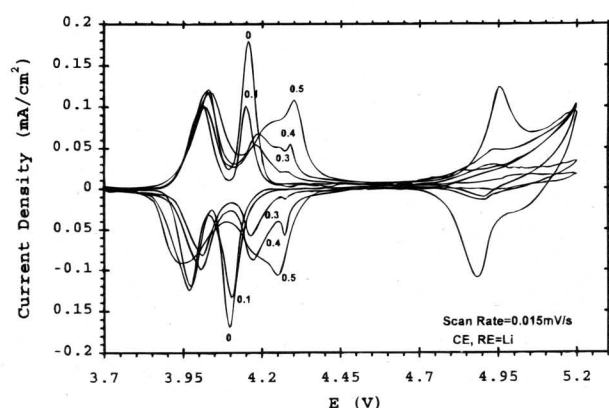
Table I summarizes the relative capacities obtained in the high-voltage region (5.1–4.5 V) and low-voltage region (4.5–3.3 V) during the third discharge. Figure 7 shows the cyclic voltammograms of the spinel series. Note that the spinel composition with the lowest copper content (LiMn<sub>1.9</sub>Cu<sub>0.1</sub>O<sub>4</sub>) provides a voltage profile and cyclic voltammogram which closely resemble those obtained from standard LiMn<sub>2</sub>O<sub>4</sub>.<sup>14</sup> As the copper content of the spinel increases, the peaks which are located at 4.05 and 4.16 V in the cyclic voltammogram of LiMn<sub>2</sub>O<sub>4</sub> (attributed to a two-step extraction of lithium from the tetrahedral 8a sites) shift to higher voltages. The higher voltage peak splits into a doublet. These features are particularly noticeable in the LiMn<sub>1.5</sub>Cu<sub>0.5</sub>O<sub>4</sub> sample in which the higher voltage peak (at 4.16 V in LiMn<sub>2</sub>O<sub>4</sub>) is shifted and split into two peaks at approximately 4.22 and 4.30 V. Although the reasons for this behavior are not yet fully understood, it is believed that the peak shifts are associated with the presence of some copper on the tetrahedral sites of the spinel structure. It is possible that one of the higher voltage peaks of the doublet may be due to oxidation of the lithium-copper-oxide impurity phase. The high-voltage reaction at 4.9 V that increases with increasing copper content is attributed to the oxidation of Cu<sup>2+</sup> to Cu<sup>3+</sup> on the octahedral (16d) sites of the spinel structure. The cyclic voltammograms indicate that all these reactions appear to be reversible.

It is clear that copper substitution has two major effects on the electrochemistry of the spinel electrode that can be interpreted in terms of the coordination and oxidation state of the copper ions. If copper substitution mimicked Amine's nickel-substituted analog, Li[Mn<sub>1.5</sub>Ni<sub>0.5</sub>]O<sub>4</sub>,<sup>16</sup> the copper ions would all be divalent and the manganese ions would be fully oxidized in a tetravalent state. In this circumstance, no charge capacity would be expected in the 3.9–4.3 V region, which originates from Mn<sup>3+</sup> → Mn<sup>4+</sup> oxidation; if the 4.9 V plateau was attributed to Cu<sup>2+</sup> → Cu<sup>3+</sup> oxidation, then a maximum capacity of 70 mAh/g would

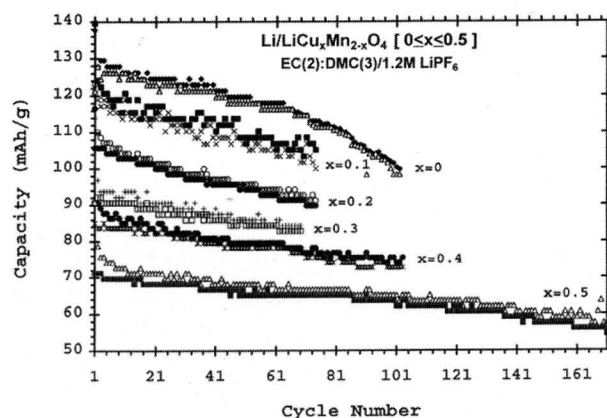
be expected at this voltage. The electrochemical data shown in Fig. 6 and 7 are clearly inconsistent with a spinel electrode with the simple cation arrangement in Li[Mn<sub>1.5</sub>Cu<sub>0.5</sub>]O<sub>4</sub>; the data imply a different cation arrangement and charge distribution in the structure of the spinel electrode. The relatively large capacity that is obtained between 3.9 and 4.4 V for LiMn<sub>2-x</sub>Cu<sub>x</sub>O<sub>4</sub> compounds with small  $x$  is associated with a large Mn<sup>3+</sup> concentration on the octahedral sites (Table I). The relatively low capacity that is obtained at 4.9 V but which increases with increasing  $x$ , and the fact that the overall achievable capacity declines sharply with increasing  $x$  is consistent with increasing Cu<sup>2+</sup> and Mn<sup>4+</sup> concentrations in the spinel samples.

Figure 8 shows the cycling performance in terms of discharge/charge capacity obtained between 5.1 and 3.3 V, expressed in mAh/g vs. cycle number for the series of LiMn<sub>2-x</sub>Cu<sub>x</sub>O<sub>4</sub> electrodes ( $0 \leq x \leq 0.5$ ). The available capacity decreases as the amount of copper in the spinel increases. However, electrodes with higher copper content showed significantly improved capacity retention during cycling. For example, Li/"LiMn<sub>1.9</sub>Cu<sub>0.1</sub>O<sub>4</sub>" cells show, on average, an initial capacity of 120 mAh/g which decreases to 103 mAh/g after 70 cycles, reflecting a 14% loss, whereas Li/"LiCu<sub>0.5</sub>Mn<sub>1.5</sub>O<sub>4</sub>" cells show an initial capacity of 71 mAh/g that fades to 65 mAh/g over the same number of cycles (8% loss). Some capacity loss (fade) may be attributed to electrolyte oxidation, particularly at potentials above 5 V.

**XANES measurements.**—Figure 9 shows the XANES spectra at the Mn K edge for Mn, MnO, Mn<sub>2</sub>O<sub>3</sub>, MnO<sub>2</sub>, and LiMn<sub>1.5</sub>Cu<sub>0.5</sub>O<sub>4</sub>. The MnO<sub>2</sub> spectra were obtained from a chemically prepared MnO<sub>2</sub> sample (CMD). Data for electrochemically prepared MnO<sub>2</sub> (EMD) are almost identical. The XANES data for LiMn<sub>1.5</sub>Cu<sub>0.5</sub>O<sub>4</sub> (dotted curve), which show a shoulder on the main peak at 11.5 eV, are consistent with the presence of both Mn<sup>4+</sup> and Mn<sup>3+</sup>, implying that Mn<sup>3+</sup> exists in a relatively low concentration in the spinel structure. The peaks in the pre-edge region (–1 to 6 eV) are due to transitions from the 1s core level to empty d states near the Fermi level. The intensity of the peaks is low because they are forbidden by the dipole selection rules. However, they are allowed by quadrupole selection rules or by hybridization p and d orbitals. This peak cannot be due to the presence of Mn<sup>2+</sup> since Mo et al.<sup>23</sup> have shown that mixtures of Mn<sup>2+</sup> and Mn<sup>4+</sup> result in a shift of the lower part of the main edge (below 0.5 eV) to lower energies than that found for MnO<sub>2</sub>. The results obtained here show a slight shift to higher energies. Figure 10 shows the XANES spectra at the Cu K edge for Cu foil, Cu<sub>2</sub>O, CuO, and LiCu<sub>0.5</sub>Mn<sub>1.5</sub>O<sub>4</sub>. The spectrum for CuO has a distinct shoulder at 8 eV. This is due to the distorted octahedral coordination of Cu. Each Cu atom is surrounded by



**Fig. 7.** Cyclic voltammogram obtained from LiCu<sub>x</sub>Mn<sub>2-x</sub>O<sub>4</sub> ( $x = 0, 0.1, 0.3, 0.4,$  and  $0.5$ ) cycled within the potential limits of 3.75–5.2 V at scan rate of 15  $\mu$ V/s. Li metal served both as counter and reference electrodes in EC(2):DMC(3)/1.2 M LiPF<sub>6</sub>.



**Fig. 8.** The cycle life behavior (charge/discharge capacity, expressed in mAh/g vs. cycle number) of LiCu<sub>x</sub>Mn<sub>2-x</sub>O<sub>4</sub> ( $0 \leq x \leq 0.5$ , in steps of  $x = 0.1$ ). Li metal served as a counter electrode in EC(2):DMC(3)/1.2 M LiPF<sub>6</sub>.

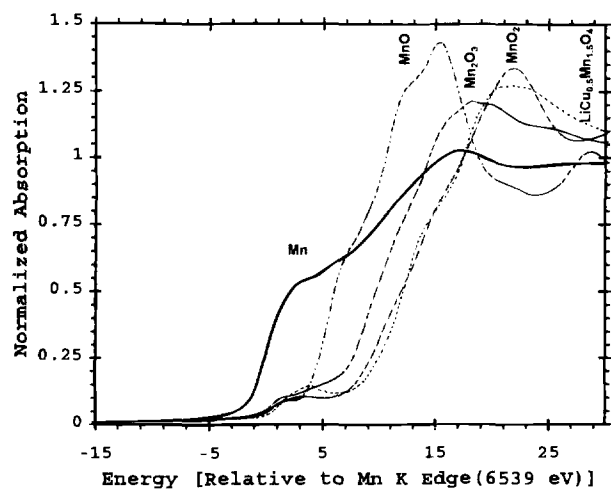


Fig. 9. Normalized Mn K edge XANES for (—) Mn, (---) MnO, (- - -) Mn<sub>2</sub>O<sub>3</sub>, (· · ·) MnO<sub>2</sub>, and (— · —) LiCu<sub>0.5</sub>Mn<sub>1.5</sub>O<sub>4</sub>.

four planar O atoms at a distance of 1.96 Å and two axial O atoms at a distance of 2.78 Å. The shoulder at 8 eV has been attributed to transitions from the 1s state to the axial 4p states and the peak at 18 eV to transitions to the planar 4p states.<sup>24</sup> In a more symmetrical coordination such as an aqueous solution of Cu<sup>2+</sup>, the shoulder at 8 eV disappears, but the position of the white-line peak at 18 eV remains unchanged.<sup>24</sup> Theoretical calculations predict that for Cu<sup>3+</sup> the white line should shift by 10 eV in going from Cu<sup>2+</sup> to Cu<sup>3+</sup>.<sup>25</sup> Measurements on KCuO<sub>2</sub>, in which the Cu<sup>3+</sup> ions have square planar coordination to neighboring, show a peak shift of only 4 eV.<sup>24</sup> Because no shift is seen in the peak and there is no shoulder in the edge, the XANES data would appear to indicate the presence of only Cu<sup>2+</sup> ions with a symmetric coordination in nominal LiMn<sub>1.5</sub>Cu<sub>0.5</sub>O<sub>4</sub>.

**Structure refinements.**—The lattice parameter *a* of LiMn<sub>2-x</sub>Cu<sub>x</sub>O<sub>4</sub> spinel structures decreases with increasing *x*, from 8.234(2) Å in LiMn<sub>2</sub>O<sub>4</sub> (*x* = 0), through 8.212(1) Å in “LiMn<sub>1.7</sub>Cu<sub>0.3</sub>O<sub>4</sub>” (*x* = 0.3) to 8.199(2) Å in “LiMn<sub>1.5</sub>Cu<sub>0.5</sub>O<sub>4</sub>” (*x* = 0.5) (Fig. 11). This trend is characteristic of an increasing concentration of Mn<sup>4+</sup> ions in the spinel structure which results from the substitution of Mn<sup>3+</sup> ions by Cu<sup>2+</sup> ions.

In a spinel structure with the cation distribution Li[Mn<sub>1.5</sub>Cu<sub>0.5</sub>O<sub>4</sub>], charge neutrality is obtained when the manganese ions are all tetravalent and the copper ions are all divalent. Replacement of copper by lithium on the octahedral sites results in Li<sub>4</sub>Mn<sub>5</sub>O<sub>12</sub> (or in spinel notation Li[Mn<sub>1.67</sub>Li<sub>0.33</sub>O<sub>4</sub>]) in which charge neutrality is achieved by

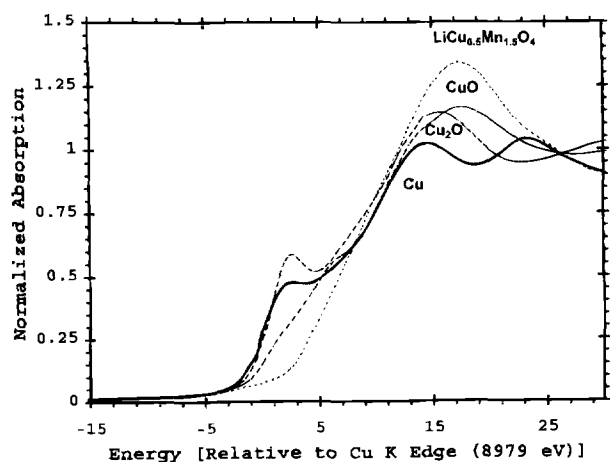


Fig. 10. Normalized Cu K edge XANES for (—) Cu foil, (---) Cu<sub>2</sub>O, (· · ·) CuO, and (— · —) LiCu<sub>0.5</sub>Mn<sub>1.5</sub>O<sub>4</sub>.

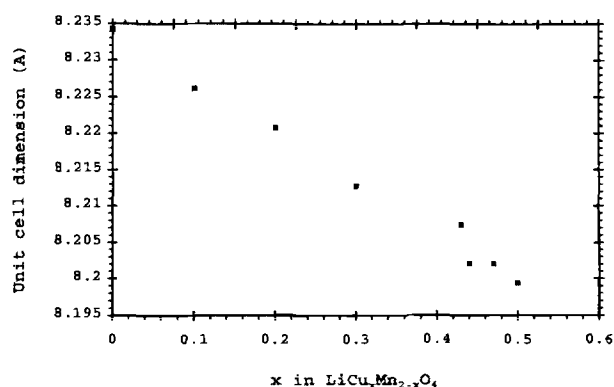


Fig. 11. Cubic cell dimension for LiCu<sub>x</sub>Mn<sub>2-x</sub>O<sub>4</sub> (0 ≤ *x* ≤ 0.55) as a function of *x*.

increasing the Mn<sup>4+</sup> content to compensate for the monovalent lithium ions. These two compounds are, in principle, the end-members of a possible solid-solution system Li[Mn<sub>1.5+x</sub>Cu<sub>0.5-3x</sub>Li<sub>2x</sub>]O<sub>4</sub> (0 ≤ *x* ≤ 0.167). In this solid-solution system it would also be possible for lithium and copper ions to exchange on the tetrahedral sites. Structural refinements of such complex systems are difficult, particularly when three different cation types are disordered over one crystallographically independent site. Despite the difficulties that were encountered in obtaining a meaningful fit to the neutron diffraction data of a two-phase reaction product, these analyses provided valuable information about the structure which could not be determined from the X-ray diffraction patterns. This information was then used for the final structure refinement with the “single-phase” X-ray diffraction data. The structure was refined by means of the prototypic cubic spinel space group Fd3m.

Because copper is a strong positive scatterer of neutrons ( $b = +0.78 \times 10^{12}$  Å), and lithium and manganese are both negative scatterers ( $b = -0.20 \times 10^{12}$  Å and  $b = -0.37 \times 10^{12}$  Å, respectively), valuable information could be obtained about the distribution of the cations in the structure from the neutron diffraction data. Structure analyses of the spinel component in two independent LiMn<sub>1.5</sub>Cu<sub>0.5</sub>O<sub>4</sub> samples with neutron diffraction data from both Argonne National Laboratory and the Rutherford Laboratory showed unequivocally, and consistently with various models, that some copper ions rather than manganese ions occupied the 8a tetrahedra with the lithium ions; the site occupancy of the copper ions was approximately 0.1. Furthermore, refinements of various models showed consistently that between 1.64 and 1.71 Mn occupied the octahedral B sites of the A[B<sub>2</sub>]O<sub>4</sub> spinel structure. Therefore, a site occupancy of 0.835, corresponding to an average 1.67 Mn in the [B<sub>2</sub>]O<sub>4</sub> spinel framework, was used for the refinement of the X-ray data. It is perhaps significant that this value corresponds to the Mn content in Li<sub>4</sub>Mn<sub>5</sub>O<sub>12</sub> (Li[Mn<sub>1.67</sub>Li<sub>0.33</sub>]O<sub>4</sub>).

The initial refinements of the X-ray data showed that the intensity of the [220] peak at approximately 31° 2θ could not be accounted for by placing only lithium on the tetrahedral sites, consistent with the neutron data. Therefore, subsequent refinements were carried out on the system (Li<sub>0.9</sub>Cu<sub>0.1</sub>)<sub>8a</sub>[Mn<sub>1.67</sub>Cu<sub>0.33-8</sub>Li<sub>1.6d</sub>]O<sub>4-α</sub> with the input from the neutron data. The parameter δ was used to control the stoichiometry of the lithium and copper on the 16d octahedral sites. A second parameter, α, was refined to determine if there was any nonstoichiometry in the oxygen content. Because of the limited number of reflections (intensity data), isotropic temperature factors (*U*) were assigned to all the ions. The cations were constrained to have the same *U* value.

The results of the refinement which yielded the best fit to the data ( $R_p = 8.7\%$ ) are summarized in Table II. The observed and calculated powder X-ray diffraction profiles of the spinel component in the LiMn<sub>1.5</sub>Cu<sub>0.5</sub>O<sub>4</sub> sample for

Table II. Crystallographic parameters of  $(\text{Li}_{0.9}\text{Cu}_{0.1})_{8a}[\text{Mn}_{1.67}\text{Cu}_{0.33-0.5}\text{Li}_{0.11}]_{16d}\text{O}_4$ <sup>a</sup>

Atom	Wyckoff notation	x	y	z	U (×100)	Site occupancy, n
Li (1)	8a	0.125	0.125	0.125	2.42(6)	0.9
Cu (1)	8a	0.125	0.125	0.125	2.42(6)	0.1
Mn (1)	16d	0.5	0.5	0.5	2.42(6)	0.835
Cu (2)	16d	0.5	0.5	0.5	2.42(6)	0.112(6)
Li (2)	16d	0.5	0.5	0.5	2.42(6)	0.053(6)
O (2)	32e	0.2652(2)	0.2652(2)	0.2652(2)	3.63(7)	1

<sup>a</sup> Space group Fd3m,  $a = 8.1923(2)$  Å; vol. 549.82(2) Å<sup>3</sup>;  $R_p$  8.7%.

this refinement are shown in Fig. 12. The lattice parameter refined to 8.1923(2) Å. Refinements of two separate samples did not favor an oxygen-deficient structure; both refinements showed that the oxygen ion positions were fully occupied ( $\alpha = 0$ ). The structure analysis showed a cation distribution  $(\text{Li}_{0.9}\text{Cu}_{0.1})_{8a}[\text{Mn}_{1.67}\text{Cu}_{0.22}\text{Li}_{0.11}]_{16d}\text{O}_4$ ; the overall composition is  $\text{Li}_{1.01}\text{Mn}_{1.67}\text{Cu}_{0.32}\text{O}_4$ . Assuming that all the copper is divalent, then the oxidation state of the manganese ions is 3.80; this finding is consistent with the XANES data that indicated only a small  $\text{Mn}^{3+}$  ion concentration in the “ $\text{LiMn}_{1.5}\text{Cu}_{0.5}\text{O}_4$ ” samples.

A spinel electrode with the composition  $(\text{Li}_{0.9}\text{Cu}_{0.1})_{8a}[\text{Mn}_{1.67}\text{Cu}_{0.22}\text{Li}_{0.11}]_{16d}\text{O}_4$  would have a theoretical capacity of 95 mAh/g, corresponding to the extraction of 0.65  $\text{Li}^+$  ions and the complete oxidation of 0.33 mol fraction  $\text{Mn}^{3+}$  to  $\text{Mn}^{4+}$  and 0.22 mol fraction  $\text{Cu}^{2+}$  to  $\text{Cu}^{3+}$ . The capacity associated with the manganese and copper ions on the octahedral sites is 48 and 32 mAh/g, respectively, which is in good agreement with the capacities of 48 and 23 mAh/g obtained from this electrode in an electrochemical cell (Table I). The experimentally achieved capacity reflects, therefore, a 75% utilization of the theoretical capacity. The possibility of exceeding this capacity appears to be limited because it is anticipated that the oxidation of  $\text{Cu}^{2+}$  ions on tetrahedral sites would occur at a voltage > 5 V, above the stability window of the electrolyte.

If all the manganese present in the precursor materials was used in the fabrication of the spinel structure, as implied by the repeated firings required to completely react the manganese oxides (Fig. 3 and 4), then the composition  $\text{Li}_{1.01}\text{Mn}_{1.67}\text{Cu}_{0.32}\text{O}_4$  indicates that 9% of the lithium and 42% of the copper in the precursor materials were not incorporated into the spinel framework. This result strongly suggests that the impurity detected in the neutron diffraction profile is a lithium copper oxide phase. Although several lithium copper oxide compounds are known to exist, particularly  $\text{Li}_2\text{O} \cdot n\text{CuO}$  compounds with divalent copper, such as  $\text{Li}_2\text{Cu}_2\text{O}_3$  ( $n = 2$ )<sup>26</sup> and  $\text{Li}_2\text{CuO}_2$  ( $n = 1$ )<sup>27</sup> none of these compounds could be indexed satisfactorily

to all the peaks of the impurity phase in the neutron diffraction pattern.

**Thermogravimetric analysis of  $\text{LiMn}_{1.5}\text{Cu}_{0.5}\text{O}_4$  under hydrogen.**—Thermogravimetric analysis measurements were conducted to investigate the thermal stability of  $\text{LiMn}_{1.5}\text{Cu}_{0.5}\text{O}_4$  relative to  $\text{LiMn}_2\text{O}_4$  under reducing conditions ( $\text{H}_2$ ) (Fig. 13). The data show significant differences, both in the onset temperature and the degree of reduction. The reduction of  $\text{LiMn}_2\text{O}_4$  that occurs through oxygen loss is initiated at approximately 140°C; over the next 200°C the sample loses 9.6% of its weight. Following a lengthy period of minimal weight loss, the material undergoes a further weight loss of 4.6% from 820 to 900°C. The first reduction process corresponds to the removal of approximately one oxygen atom from the spinel formula unit, resulting in “ $\text{LiMn}_2\text{O}_3$ ” (the theoretical weight loss for this reaction is 8.9%). The total weight loss of 14.2% corresponds closely to the formation of “ $\text{LiMn}_2\text{O}_{2.5}$ ,” alternatively “ $\text{Li}_2\text{O} \cdot 4\text{MnO}$ ” (the theoretical weight loss for this reaction is 13.3%).

Inclusion of copper in the spinel framework dramatically increases the reactivity toward hydrogen. The onset of weight loss was almost immediate, and at 230°C the  $\text{LiMn}_{1.5}\text{Cu}_{0.5}\text{O}_4$  sample had lost 26% of its initial weight, indicating that the residue had the empirical formula  $\text{LiMn}_{1.5}\text{Cu}_{0.5}\text{O}_{1.0}$ . Subsequent heating to 900°C resulted in an additional 3.5% weight loss, mostly above 750°C. The result indicates that the reduced product of  $\text{LiMn}_{1.5}\text{Cu}_{0.5}\text{O}_4$  at 900°C is comprised essentially of metallic Cu and Mn, and  $\text{Li}_2\text{O}$  (the theoretical weight loss for the reaction is 30.2%). Moreover, the result demonstrates that the presence of copper in the spinel greatly facilitates electron transfer within the spinel framework, which at moderate temperatures (200–300°C), leads to an almost complete reduction of  $\text{LiMn}_{1.5}\text{Cu}_{0.5}\text{O}_4$ .

## Conclusions

Novel electroactive materials,  $\text{LiMn}_{2-x}\text{Cu}_x\text{O}_4$ , ( $0.1 \leq x \leq 0.5$ ) have been prepared and evaluated in lithium cells. The data show that lithium can be extracted from the spinel

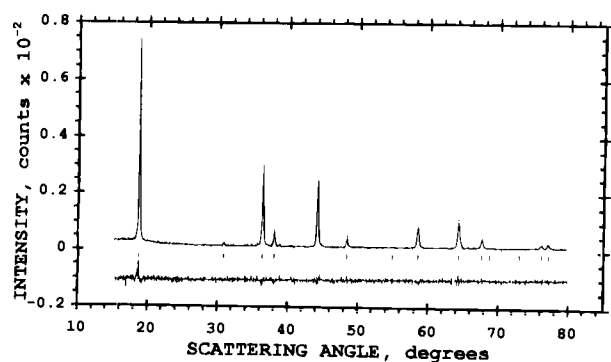


Fig. 12. Powder X-ray diffraction pattern of  $\text{LiMn}_{1.5}\text{Cu}_{0.5}\text{O}_4$  using  $\text{CuK}$ . The structure was refined with the prototypic cubic spinel space group Fd3m. The observed data points are depicted as small dots, and the line through them is the calculated pattern based on the refined model. The difference between the observed and calculated patterns is shown below the profiles.

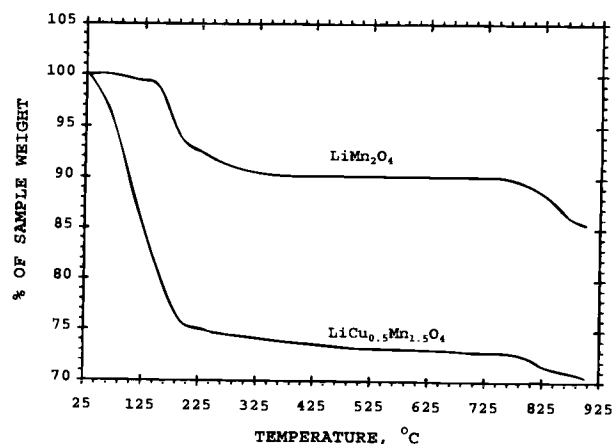


Fig. 13. TGA profiles (30–900°C at 5°C/min in  $\text{H}_2$ ) of  $\text{LiMn}_2\text{O}_4$  and  $\text{LiCu}_{0.5}\text{Mn}_{1.5}\text{O}_4$ .

structures in two main potential regions: 3.9–4.3 V and 4.8–5.0 V, attributed to the oxidation of  $Mn^{3+}$  to  $Mn^{4+}$  and  $Cu^{2+}$  to  $Cu^{3+}$ , respectively. The reactions are reversible. Stable electrochemical cycling has been observed for electrode compositions with high values of  $x$  but with low capacity (60–70 mAh/g), for example, in an electrode with overall composition " $LiMn_{1.5}Cu_{0.5}O_4$ " ( $x = 0.5$ ). Analysis of X-ray and neutron diffraction data and XANES spectra revealed that it is difficult to synthesize single-phase lithium-copper-manganese-oxide spinel compounds with a predetermined composition. The stability and relatively low reactivity of CuO (compared to  $Li_2O$ ) appears to restrict the complete incorporation of copper into the spinel structure. The cation distribution in these spinel structures is highly complex, which makes it difficult to perform detailed structure analyses with X-ray and neutron diffraction data with a high degree of accuracy. Although the XANES data show that the oxidation state of copper in these spinel compounds is divalent, the possibility of a small amount of  $Cu^{1+}$  (in tetrahedral sites) or  $Cu^{3+}$  (in octahedral sites) in the starting spinel structures should not be entirely discounted. In situ XANES and X-ray diffraction experiments are being planned in order to obtain further information about the structural properties of these spinel compounds.

### Acknowledgments

This work was performed under an SBIR Phase I DoD program sponsored by the U.S. Army CECOM, administered by the Army Research Laboratory, Fort Monmouth, NJ, under Contract No. DAAB07-97-C-D304. Support for Argonne National Laboratory from the U.S. Department of Energy's Advanced Battery Program, Chemical Sciences Division, Office of Basic Energy Sciences, under Contract No. W-31-109-Eng-38, is gratefully acknowledged. The XAS measurements were done at Beam Line X11A at NSLS. This work was supported by the Assistant Secretary for Energy Efficiency and Renewable Energy, Office of Transportation Technologies, Electric and Hybrid Propulsion Division, U.S. Department of Energy under Contract No. DE-AC02-76CH00016. Dr. W. I. F. David and Dr. R. M. Ibberson are thanked for collecting neutron diffraction data at the Rutherford Appleton Laboratory and for undertaking some preliminary structural refinements. The authors thank J. H. Hemenway and R. Laura for assisting in manuscript preparation and Professor J. B. Goodenough for stimulating discussions.

Manuscript submitted October 23, 1997; revised manuscript received December 12, 1997.

Covalent Associates assisted in meeting the publication costs of this article.

### REFERENCES

- J. R. Dahn, T. Zheng, Y. Liu, and J. S. Xue, *Science*, **270**, 590 (1995).
- R. Yazami, presented at the 12th International Seminar, Primary and Secondary Battery Technology and Applications, Deerfield Beach, FL, March 6–9, 1995.
- Y. Idota, T. Kubota, A. Matsufuji, Y. Maekawa, and T. Miyasaki, *Science*, **276**, 1395 (1997).
- J. B. Goodenough, D. G. Wickham, and W. J. Croft, *J. Phys. Chem. Solids*, **5**, 107 (1958).
- K. Mizushima, P. C. Jones, P. J. Wiseman, and J. B. Goodenough, *Mater. Res. Bull.*, **15**, 783 (1980).
- E. Plitcha, M. Salomon, S. Slane, M. Uchiyama, D. Chua, W. B. Ebner, and H. W. Lin, *J. Power Sources*, **21**, 25 (1987).
- J. R. Dahn, U. von Sacken, and C. A. Michal, *Solid State Ionics*, **44**, 87 (1990).
- A. Leecerf, M. Broussely, and J. P. Gabano, U.S. Pat. 4,980,080 (1989).
- T. Nagaura, *JEC Battery Newsletter*, **2**, March/April (1991).
- ITE Battery Newsletter, No. 6 (Nov–Dec) (1996).
- M. M. Thackeray, *Progress in Batteries and Battery Materials*, Vol. 14, R. J. Brodd, Editor, p 1, ITE Press, Inc., Brunswick, OH (1995), and references therein.
- R. J. Gummow, A. de Kock, D. C. Liles, and M. M. Thackeray, *Solid State Ionics*, **69**, 59 (1994).
- G. Pistoia, C. Bellito, and A. Antonini, Abstract 824, p 1011, The Electrochemical Society Meeting Abstracts, Vol. 96-2, San Antonio, TX, Oct 6–11, 1996.
- A. D. Robertson, S. H. Lu, and W. F. Howard, Jr., *J. Electrochem. Soc.*, **144**, 3505 (1997).
- I. J. Davidson, R. S. McMillan, and J. J. Murray, U.S. Pat. 5,370,949 (1994).
- K. Amine, H. Tukamoto, H. Yasuda, and Y. Fujita, Abstract 70, p 114, The Electrochemical Society Meeting Abstracts, Vol. 95-2, Chicago, IL, Oct. 8–13, 1995; K. Amine, H. Tukamoto, H. Yasuda, and Y. Fujita, *J. Electrochem. Soc.*, **143**, 1607 (1996).
- C. Sigala, D. Guyomard, A. Verbaere, Y. Piffard, and M. Tournoux, *Solid State Ionics*, **81**, 167 (1995).
- Y. Gao, K. Myrtle, M. Zhang, J. N. Reimers, and J. R. Dahn, *Phys. Rev. B*, **54**, 3878 (1996).
- Y. Ein-Eli and W. F. Howard, Jr., *J. Electrochem. Soc.*, **144**, L205 (1997).
- K. I. Pandya, R. W. Hoffman, J. McBreen, and W. E. O'Grady, *J. Electrochem. Soc.*, **137**, 383 (1990).
- J. Wong, F. W. Lytle, R. P. Mssmer, and D. H. Maylotte, *Phys. Rev. B*, **30**, 5596 (1984).
- A. C. Larson and R. B. Von Dreele, *GSAS-General Structure Analysis System*, Rept. LA-UR-86-748, Los Alamos National Laboratory, Los Alamos, NM (1990).
- Y. Mo, Y. Hu, I. T. Bae, B. Miller, M. R. Antonio, and D. A. Scherson, *J. Electrochem. Soc.*, **144**, 1598 (1997).
- J. M. Tranquada, S. M. Heald, and A. R. Moodenbaugh, *Phys. Rev. B*, **36**, 5263 (1987).
- E. E. Alp, G. K. Shenoy, D. G. Hinks, D. W. Capone II, L. Soderholm, H. B. Schuttler, J. Guo, D. E. Ellis, P. A. Montano, and M. Ramanathan, *Phys. Rev. B*, **35**, 7199 (1987).
- JCPDS Data File 36-661, Swarthmore, PA.
- J. Barker and M. Yazid Saidi, U.S. Pat. 5,670,277 (1997).